Excited state surfaces in density functional theory: A new twist on an old problem

Paul Wiggins, J. A. Gareth Williams, and David J. Tozer[a)]
Department of Chemistry, Durham University, South Road, Durham DH1 3LE, United Kingdom

(Received 6 July 2009; accepted 14 August 2009; published online 1 September 2009)

Excited state surfaces in density functional theory and the problem of charge transfer are considered from an orbital overlap perspective. For common density functional approximations, the accuracy of the surface will not be uniform if the spatial overlap between the occupied and virtual orbitals involved in the excitation has a strong conformational dependence; the excited state surface will collapse toward the ground state in regions where the overlap is very low. This characteristic is used to predict and to provide insight into the breakdown of excited state surfaces in the classic push-pull 4-(dimethylamino)benzonitrile molecule, as a function of twist angle. The breakdown is eliminated using a Coulomb-attenuated functional. Analogous situations will arise in many molecules. © *2009 American Institute of Physics*. [doi:10.1063/1.3222641]

Time-dependent density functional theory (TDDFT)[1,2] in the adiabatic approximation is extensively used in the study of excited states, providing theoretical insight into the electronic and optical properties of molecules. The accuracy of a TDDFT calculation is largely governed by the choice of exchange-correlation functional and there is a large body of literature quantifying the accuracy of common density functional approximations (DFAs). Their most serious deficiency is arguably the underestimation of charge-transfer (CT) excitation energies,[3–10] which limits their utility in fields such as organic electronics and photonics, molecular exciplexes, and photovoltaics. It is vital to understand when these problems occur and how they may be overcome.

In a recent study,[8] we attempted to put the CT problem onto a more quantitative basis. We defined a parameter that measures the degree of spatial overlap between the occupied and virtual orbitals involved in an excitation and examined how it correlates with the accuracy of the excitation energy. A broad correlation was observed for both generalized gradient approximations (GGAs) and hybrid functionals, being less pronounced in the latter. In particular, when the overlap dropped too low then excitations became significantly underestimated, leading us to propose that low overlap should be used in a diagnostic manner to identify the problematic excitations. We also demonstrated that the breakdown is eliminated using a Coulomb-attenuated DFA,[11–13] which introduces an increased amount of nonlocal, exact exchange at long range.

The real potential of TDDFT lies in the ability to calculate excited state potential energy surfaces, by evaluating the sum of the vertical excitation energy and the ground state energy, as a function of nuclear conformation. Analytic gradient techniques[14,15] can then be used to determine minimum energy paths and stationary points on these surfaces. The CT deficiency in common DFAs manifests itself as an error in these surfaces.[9,10,16,17] For example, Plötner and Dreuw[9] observed an artificial minimum in their study of a fluorescent yellow pigment, which they explicitly attributed to the strong CT-character of that conformation.

In this communication, we consider excited state surfaces and the associated CT problem from the orbital overlap perspective of Ref. 8. For common DFAs, the implications of this earlier study are simple: If the spatial overlap between the occupied and virtual orbitals involved in the excitation has a strong dependence on the nuclear conformation, then the accuracy of the surface will not be uniform and its topography—and associated molecular structures—will be incorrect. Specifically, if the overlap drops too low in a particular region of nuclear conformation space, then the excitation energies will be significantly underestimated and the excited state surface will collapse toward the ground state surface in that region. We shall demonstrate that this characteristic can be used to predict and provide insight into the breakdown of excited state surfaces in the classic, push-pull molecule, 4-(dimethylamino)benzonitrile (DMABN) in Fig. 1. We shall subsequently demonstrate that the breakdown is eliminated using a Coulomb-attenuated functional. Analogous results are to be expected in *any* molecule where conformational changes reduce spatial orbital overlap sufficiently, including the wide variety of technologically important CT molecules based on the same donor-benzene-acceptor motif.

DMABN has been extensively studied due to its dual fluorescence.[18] In addition to the emission from a locally excited (LE) state, the molecule exhibits an anomalous emission, attributed to an intramolecular CT (ICT) state. Following Rappoport and Furche[16] and to aid clarity in the present

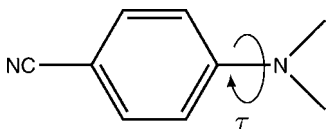

FIG. 1. Twist coordinate in DMABN.

[a)]FAX: +44 191 384 4737. Electronic mail: d.j.tozer@durham.ac.uk.

study, we shall label the two excited state surfaces by LE and ICT although, as will be seen, this classification is not always appropriate. Several models have been proposed to explain the dual fluorescence and many experimental and theoretical studies have been carried out.[18] Of particular note is the work of Köhn and Hättig,[17] who used the resolution of the identity second-order approximate coupled cluster (RI-CC2) method,[19] with an extensive triple zeta TZVPP basis set,[20,21] to study the variation in the ICT and LE singlet surfaces as a function of the CNCC dimethylamino twist angle, denoted τ, in Fig. 1. This is the key coordinate in the twisted intramolecular charge transfer (TICT) model of dual fluorescence.[22] These authors used analytic gradient techniques to calculate RI-CC2 minimum energy structures on the two excited state surfaces, for a series of constrained twist angles in C_2 symmetry. Their resulting energy surfaces are reproduced[23] in Fig. 2(a); the ICT and LE states transform as A and B symmetry species, respectively, under this point group. Consistent with the TICT model, the energy of the ICT state drops as the molecule twists, reaching a minimum at $\tau=90°$. The LE state decreases to a shallow minimum at $\tau=19°$ and then increases to a maximum at $\tau=90°$.

The RI-CC2 study of Köhn and Hättig[17] is the most theoretically advanced study of DMABN performed to date and so we use it as a benchmark, against which TDDFT results can be compared. In order to allow direct comparison with the benchmark ICT and LE energies, all TDDFT calculations in the present study were determined at the respective RI-CC2 geometries[23] of Ref. 17, with the same TZVPP basis set. Following Ref. 8, the degree of spatial overlap between the occupied and virtual orbitals involved in each excitation was quantified using the parameter

$$\Lambda = \frac{\Sigma_{i,a}\kappa_{ia}^2 O_{ia}}{\Sigma_{i,a}\kappa_{ia}^2}, \tag{1}$$

where O_{ia} is the inner product of the moduli of individual unperturbed occupied and virtual Kohn–Sham orbitals, φ_i and φ_a,

$$O_{ia} = \langle |\varphi_i||\varphi_a| \rangle = \int |\varphi_i(\mathbf{r})||\varphi_a(\mathbf{r})| d\mathbf{r}, \tag{2}$$

and

$$\kappa_{ia} = X_{ia} + Y_{ia} \tag{3}$$

is a measure of the contribution of the "ia" occupied-virtual pair to the excitation. The matrices $\mathbf{X}$ and $\mathbf{Y}$ are the solutions to the usual TDDFT generalized eigenvalue problem.[1,2] All calculations were performed using the DALTON (Ref. 24) program.

The first category of DFA we consider is the GGA, which does not include any nonlocal, exact exchange. We use the Perdew–Burke–Ernzerhof (PBE) variant,[25] but expect all GGAs to perform similarly. Figure 3 shows the variation in Λ for the ICT and LE excitations, as a function of τ. The values drop markedly as τ approaches 90°, both falling well below the diagnostic test threshold[8] of ~0.4. We therefore expect both excitation energies to become increasingly underestimated as the molecule twists, causing both

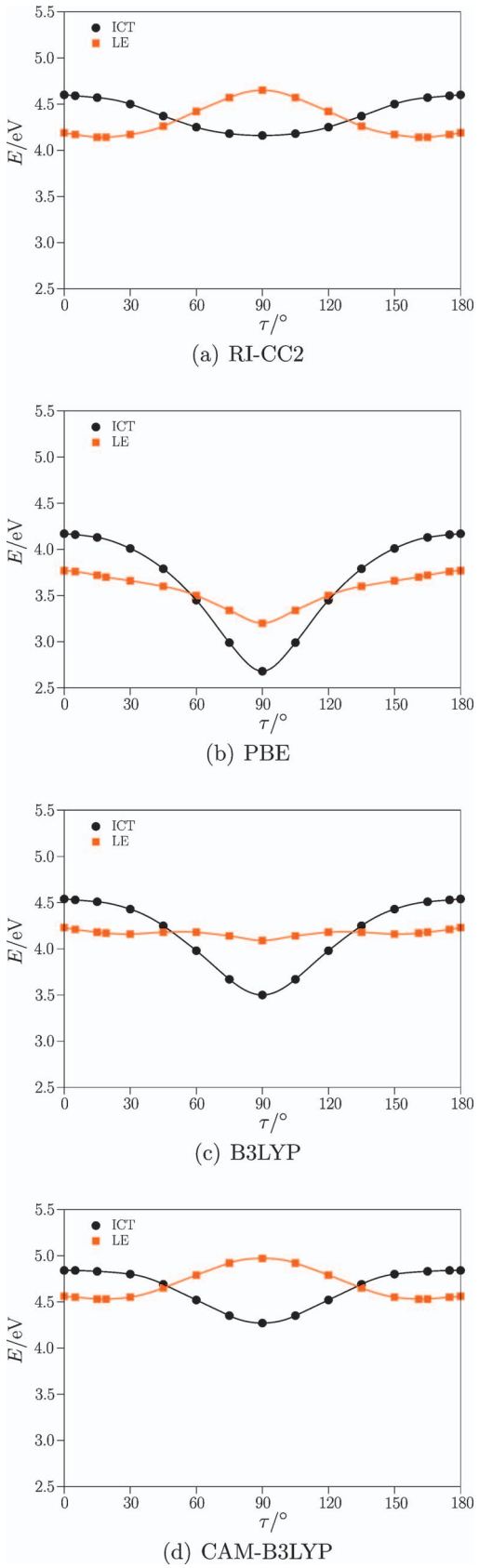

FIG. 2. Singlet excited state surfaces in DMABN, plotted as a function of twist angle τ, determined using (a) RI-CC2, (b) PBE, (c) B3LYP, and (d) CAM-B3LYP. Energies are quoted relative to the energy of the ground state minimum structure, determined using each method. RI-CC2 results from Ref. 17.

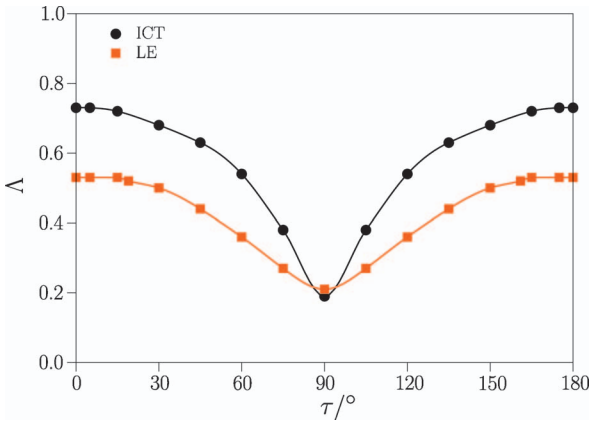

FIG. 3. Spatial orbital overlap Λ for ICT and LE excitation energies, plotted as a function of twist angle τ, determined using PBE.

excited state surfaces to increasingly collapse toward the ground state. This is exactly what happens in Fig. 2(b), which plots the PBE excited state surfaces. For the ICT state, which should (according to RI-CC2) drop in energy as τ approaches 90°, the effect of the breakdown is to lower the surface far too much upon twisting. There is still a single minimum at τ=90°, but it occurs 1.5 eV below RI-CC2. For the LE state, which should decrease to a shallow minimum then increase to a maximum at τ=90°, the effect of the breakdown is to completely change the topography. No shallow minimum is observed; it drops monotonically to a minimum at τ=90°, with an energy again 1.5 eV below RI-CC2. The differences between PBE and RI-CC2 energies at τ =90° are more than three times larger than the differences at τ=0°, consistent with Fig. 3.

The orbital overlap perspective provides a simple explanation as to why *both* excited state surfaces break down upon twisting, whereas one might intuitively expect only the "CT" state to do so. The ICT and LE excitations are dominated by single orbital transitions from the highest occupied molecular orbital (HOMO) to the lowest unoccupied molecular orbital (LUMO) or LUMO+1, depending on twist angle and functional. The quantity Λ is therefore a measure of how well these orbitals overlap in space. Figure 4 plots these dominant transitions at twist angles of 0° and 90°. At τ=0°, the HOMO overlaps well with both virtual orbitals and so both excitations exhibit reasonably large Λ values; the overlap is visibly larger for the ICT excitation, consistent with Fig. 3. Upon twisting to 90°, the virtual orbitals barely change, whereas the HOMO localizes on the dimethylamino group (as expected from simple chemical and symmetry arguments). The overlap between the HOMO and both virtual orbitals therefore reduces significantly and so both Λ values become small, to the detriment of *both* excited state surfaces. The LE classification is clearly inappropriate at this twisted geometry.

The second category of DFA we consider is the hybrid functional, which includes a global fraction (~20%) of nonlocal, exact exchange. We consider the ubiquitous B3LYP functional,[26,27] but expect other hybrids to perform similarly.

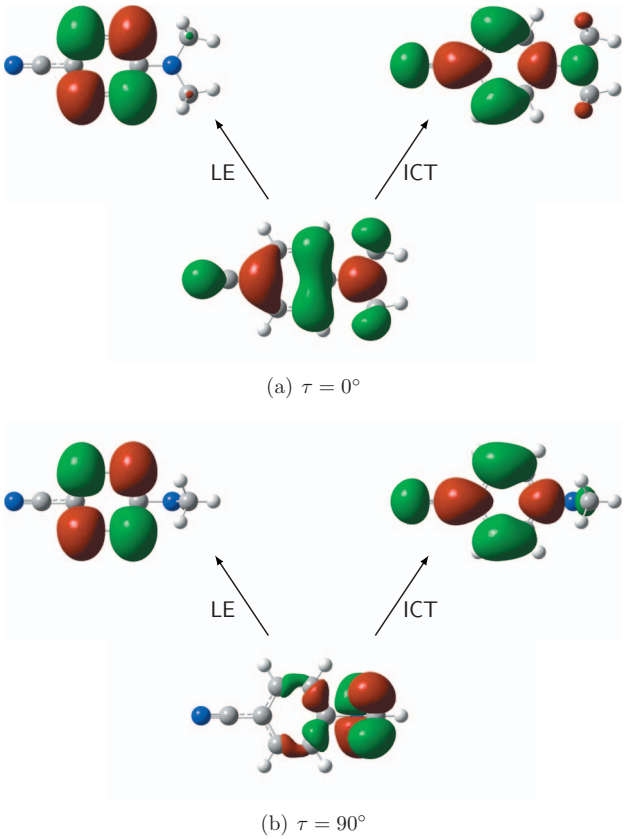

FIG. 4. Dominant orbital transitions at twist angles of (a) 0° and (b) 90°, determined using PBE. Virtual orbitals were calculated at the respective RI-CC2 ICT and LE geometries. The HOMO was calculated at the RI-CC2 (a) LE and (b) ICT geometry; it looks essentially identical when the alternative geometry is instead used.

We note that B3LYP minimum energy surfaces have previously been presented by Rappoport and Furche.[16] Our B3LYP Λ values and orbital plots (not presented) are very similar to those of PBE. We therefore expect both surfaces to again break down upon twisting, but to a lesser extent than with PBE. Figure 2(c) presents the B3LYP excited state surfaces, which are essentially indistinguishable from those of Ref. 16. As expected, B3LYP is intermediate between PBE and RI-CC2. As τ approaches 90°, the ICT surface again drops too low. The LE surface does now exhibit a shallow minimum, but at too large a twist angle. With increasing twist, the surface again breaks down, yielding a minimum at τ=90°. The authors of Refs 16 and 17 commented on the high exothermicity of the LE→ICT reaction with B3LYP. The latter commented on the "erroneously nearly constant minimum path" of the LE state. These observations are readily understood from the orbital overlap perspective.

The third category of DFA we consider is the Coulomb-attenuated functional, containing an increased fraction of nonlocal, exact exchange at long range. We consider the CAM-B3LYP variant,[13] but others should perform similarly. Figure 2(d) presents the CAM-B3LYP excited state surfaces. The topographical agreement with RI-CC2 is striking; there is no breakdown. The LE→ICT exothermicity is reduced significantly compared to PBE and B3LYP. The LE surface

exhibits a shallow minimum at the same twist angle as RI-CC2 and a maximum at 90°. We do note, however, that the CAM-B3LYP energies are always above RI-CC2, the difference being larger for the LE state. At small twist angles, B3LYP is closer to RI-CC2, consistent with the $\tau=0°$ results in Ref. 28.

For the ICT state at $\tau=90°$, Köhn and Hättig[17] observed that their RI-CC2 structure (C_{2v} symmetry) was actually a saddle point and that the symmetry breaking coordinate was a pyramidalization of the carbon atom adjacent to the dimethylamino group. The energy of the resulting C_s structure was just 0.1 eV below the C_{2v} structure. All three DFT functionals instead predict this C_s structure to be higher in energy than the C_{2v} structure, by 0.25, 0.14, and 0.03 eV for PBE, B3LYP, and CAM-B3LYP, respectively. The discrepancy in energy ordering between PBE/B3LYP and RI-CC2 is again consistent with an orbital overlap perspective: pyramidalization from C_{2v} to C_s increases the PBE/B3LYP Λ value from 0.19 to 0.28 and so the excitation energy at the former structure is likely to be more underestimated, leading to a lower energy.

In this communication, we presented a striking example of the breakdown of TDDFT excited state surfaces from common DFAs. We have shown that a simple orbital overlap analysis can be used to predict and provide insight into the breakdown and demonstrated that the breakdown is eliminated using a Coulomb-attenuated functional. We illustrated these ideas by twisting the classic push-pull DMABN molecule, which is sufficiently small to allow RI-CC2 to be used. Analogous situations will arise in many molecules, including larger CT molecules based on the donor-benzene-acceptor motif. With increasing molecular size, RI-CC2 will rapidly become impractical due to its high computational cost. TDDFT will be the only practical approach and the findings of the present study—particularly the improved results from Coulomb-attenuated functionals—will be pertinent.

We are very grateful to Andreas Köhn and Christof Hättig for providing the RI-CC2 excited state structures and energies of Ref. 17.

[1] E. Runge and E. K. U. Gross, Phys. Rev. Lett. **52**, 997 (1984).
[2] M. E. Casida, *Recent Advances in Density Functional Methods, Part I* (World Scientific, Singapore, 1995), pp. 155–192.
[3] D. J. Tozer, R. D. Amos, N. C. Handy, B. O. Roos, and L. Serrano-Andrés, Mol. Phys. **97**, 859 (1999).
[4] A. Dreuw, J. L. Weisman, and M. Head-Gordon, J. Chem. Phys. **119**, 2943 (2003).
[5] D. J. Tozer, J. Chem. Phys. **119**, 12697 (2003).
[6] O. Gritsenko and E. J. Baerends, J. Chem. Phys. **121**, 655 (2004).
[7] T. Ziegler, M. Seth, M. Krykunov, and J. Autschbach, J. Chem. Phys. **129**, 184114 (2008).
[8] M. J. G. Peach, P. Benfield, T. Helgaker, and D. J. Tozer, J. Chem. Phys. **128**, 044118 (2008).
[9] J. Plötner and A. Dreuw, Chem. Phys. **347**, 472 (2008).
[10] M. Wanko, M. Garavelli, F. Bernardi, T. A. Niehaus, T. Frauenheim, and M. Elstner, J. Chem. Phys. **120**, 1674 (2004).
[11] T. Leininger, H. Stoll, H.-J. Werner, and A. Savin, Chem. Phys. Lett. **275**, 151 (1997).
[12] H. Iikura, T. Tsuneda, T. Yanai, and K. Hirao, J. Chem. Phys. **115**, 3540 (2001).
[13] T. Yanai, D. P. Tew, and N. C. Handy, Chem. Phys. Lett. **393**, 51 (2004).
[14] F. Furche and R. Ahlrichs, J. Chem. Phys. **117**, 7433 (2002).
[15] C. V. Caillie and R. D. Amos, Chem. Phys. Lett. **317**, 159 (2000).
[16] D. Rappoport and F. Furche, J. Am. Chem. Soc. **126**, 1277 (2004).
[17] A. Köhn and C. Hättig, J. Am. Chem. Soc. **126**, 7399 (2004).
[18] Z. R. Grabowski, K. Rotkiewicz, and W. Rettig, Chem. Rev. (Washington, D.C.) **103**, 3899 (2003).
[19] C. Hättig and F. Weigend, J. Chem. Phys. **113**, 5154 (2000).
[20] A. Schäfer, C. Huber, and R. Ahlrichs, J. Chem. Phys. **100**, 5829 (1994).
[21] F. Weigend, M. Häser, H. Patzelt, and R. Ahlrichs, Chem. Phys. Lett. **294**, 143 (1998).
[22] Z. R. Grabowski, K. Rotkiewicz, and A. Siemiarczuk, Nouv. J. Chim. **3**, 443 (1979).
[23] A. Köhn, private communication (February 26, 2009).
[24] DALTON, a molecular electronic structure program, Release 2.0, 2005, see http://www.kjemi.uio.no/software/dalton/dalton.html.
[25] J. P. Perdew, K. Burke, and M. Ernzerhof, Phys. Rev. Lett. **77**, 3865 (1996).
[26] A. D. Becke, J. Chem. Phys. **98**, 5648 (1993).
[27] C. Lee, W. Yang, and R. G. Parr, Phys. Rev. B **37**, 785 (1988).
[28] M. J. G. Peach, A. J. Cohen, and D. J. Tozer, Phys. Chem. Chem. Phys. **8**, 4543 (2006).